MATERIALE PLASTICE
https://revmaterialeplastice.ro
https://doi.org/10.37358/Mat.Plast.1964

Synthesis of Ethylenediaminetetraacetic Acid-Functionalized Chitosan Cryogels as Potential Sorbents of Heavy Metal Ions

MARIA MARINELA LAZAR[1*], IONEL ADRIAN DINU[1,2], MARIA VALENTINA DINU[1]
[1]"Petru Poni" Institute of Macromolecular Chemistry, Department of Functional Polymers, 41A Grigore Ghica Voda Alley, 700487, Iasi, Romania
[2] Department of Chemistry, University of Basel, BioPark Rosental (BPR) 1096, Mattenstrasse 24a, 4058 Basel, Switzerland

Abstract: *An original functionalization strategy is proposed here to design chitosan (CS)-based cryogels with ethylenediaminetetraacetic acid (EDTA) moieties. Cryogels with aligned micro-sized tubular structures were further engineered through an unidirectional freezing approach. Attachment of EDTA groups onto CS chains was proved by ^{1}H-RMN and FT-IR spectroscopy. The formation of EDTA-functionalized 3D porous CS-based cryogels was demonstrated by several methods of characterization (FTIR spectroscopy, optical microscopy, SEM, porosity measurements, swelling behavior, copper (II) retention capacity). The sorption tests pointed out the high potential of EDTA-functionalized CS-based cryogels for heavy metal ions retention.*

Keywords*: chitosan, cryo-beads, functionalization, heavy metal ions, sorption kinetics*

1. Introduction

Lately, biopolymers have been intensively harnessed to design more cost effective eco-friendly sorbents. Compared to conventional adsorbents such as activated carbon (AC) or synthetic ion exchangers, biopolymers represent valuable alternatives for sorption of various contaminants [1-3]. Consequently, over the years numerous biopolymers have been used as main matrix to develop composite-based sorbents for removal of heavy metal ions (HMIs) [4-6], dyes [7,8], or other pollutants [9,10]. One of the most promising biopolymers is chitosan (CS), a low-cost renewable polycation which is obtained from shells of crustaceans (crabs, shrimps, lobsters, etc.) by acidic and alkaline treatments. The -NH_2 groups of CS are strongly reactive and responsible for HMIs chelation [2]. To overcome dissolution of CS at pH < 5.5, its chemical cross-linking with glutaraldehyde, epichlorohydrin, benzoquinone or ethylene glycol diglycidyl ether [2,3,11-13] or its blending with other natural or synthetic polymers or inorganic materials [14,15] has been proposed. In addition, CS has been easily modified by grafting ligand moieties to the -NH_2 or -OH groups. For instance, functionalization with amidoxime [16-18], thiosemicarbazide [19], thiourea [20], aminopolycarboxylic acid (APCAs) [21-28], thymine [10], polydopamine [29], and aminophosphonate [30] moieties allowed designing of CS derivatives with targeted selectivity for various HMIs. The amidoxime-functionalized CS was used for removal and recovery of uranium [16,17], APCAs-functionalized CS derivatives were studied for the uptake and recovery of lead [21,25,28], nickel [22,23], cobalt [23], rare earths [24], or copper [27], while polydopamine-modified CS was efficient for removal of chromium(VI) and organic dyes [29]. APCAs-functionalized CS derivatives have been also investigated as a stationary phase in liquid chromatography for the separation of HMIs mixtures [22,24]. Roosen and Binnemans [24] have investigated the potential of a APCAs-functionalized CS/silica derivative for the separation of Nd^{3+}/Ho^{3+}, Pr^{3+}/Nd^{3+} and $Pr^{3+}/Nd^{3+}/Ho^{3+}$ mixtures from dilute nitric acid solutions with medium pressure liquid chromatography. Nevertheless, in most of these research studies, it has been mentioned the low-cost, the availability from natural resources, and high metal ion loading capacity as the main advantages of functionalized CS derivatives. To fully exploit their feasibility for treatment of HMIs-containing wastewaters, their regeneration in mild conditions, a fast rate of pollutant sorption/desorption, and a high level of reusability should be taken under consideration when new sorbents are planned to be developed. In this regard, we

* *email: mariperju@icmpp.ro*

proposed here the synthesis of ethylenediaminetetraacetic acid (EDTA)-functionalized CS cryogels, as beads, with the main to address some of the limitations of the already reported analogues including water soluble CS derivatives or conventional hydrogels. Polymer-based materials in cryogel form are highly recommended because of their facile synthesis (water as a solvent), macroporous 3D structure, high mechanical stability, interconnected flow-channels allowing the study of viscous organic mobile phase even at high flow rates without any pressure drop and diffusion-related issues [31-33]. Herein, the ice-segregation-induced self-assembly technique or cryogenic process was applied to obtained CS-based micro-structured frameworks with an oriented lamellar architecture achieved by the additional use of unidirectional freezing in nitrogen liquid (LN). To improve the 'active' surface area of our CS-based cryogels, the chemically modification of CS with EDTA coordinating groups was further carried out. The impact of the synthesis strategy on the CS-based cryogels sorption properties was also investigated by performing sorption kinetics and reusability studies towards Cu^{2+} ions.

2. Materials and methods

2.1. Materials

CS, as powder, glutaraldehyde (GA) solution (Grade I, 25% in H_2O), 4,4'–Ethylenebis(2,6– morpholinedione) (EDTA dianhydride), and copper(II) chloride dihydrate ($CuCl_2 \cdot 2H_2O$), purchased from Sigma-Aldrich (GmbH, Germany), were used without any further purification.

The deacetylation degree (DD) of CS was first evaluated by FTIR spectroscopy, as previously shown [34]. It was determined that CS has 85% deacetylated units. The DD value of CS was further confirmed by ^{1}H-RMN spectroscopy taking into consideration the value of the integral of the signal at 2.05 ppm, attributed to the methyl protons in the acetyl group, respectively that of the signal at 3.18 ppm corresponding to the proton bound to the carbon atom C2 in the pyranose ring, CH-NH_2 [35]. The molar mass (M_v) of CS was assessed by viscometry [36], and was calculated as 341 kDa.

Hydrochloric acid, sodium hydroxide, acetic acid, methanol, and isoproponal of the highest commercially purity, provided by Chemical Company, were used as received.

2.2. Methods

2.2.1. Synthesis of CS-based cryobeads

To prepare chemically cross-linked CS cryobeads, the cross-linking of CS with GA was conducted at −18°C within the millimeter-sized droplets, according to a procedure previously reported [4,37] with some modifications. Typically, 0.2 g of CS powder was dissolved in 10 mL of 2 wt.% CH_3COOH aqueous solution and then the aqueous solution of GA (0.32 mL, 5 wt.%) was dropwise added under vigorous stirring over 30 min. Then, the mixture was kept under stirring 1 h in an ice bath. Finally, the homogeneous dispersion was added drop-by-drop, with an Eppendorf pipette, in LN (Step 1 – Scheme 1). The size of the frozen droplets was easily controlled by the tip diameter of the Eppendorf pipettes. Afterwards, the frozen droplets were separated from LN and immediately transferred in an Arctiko Freezer at −18 °C to ensure the complete cross-linking of CS by GA. After 24 h, the CS cryobeads were thawed at room temperature (RT) and washed several times with MilliQ water. Thereafter, the CS cryobeads were freeze-dried in a LABCONCO FreeZone apparatus for 48 h, at –50°C and 0.04 mbars. The gel fraction yield (*GFY*, %) was determined by Eq. (1) [38]:

$$GFY(\%) = \frac{W_d}{W_m} \times 100 \quad (1)$$

where: W_d is the weight of the freeze-dried cryobeads; W_m is the total amount of CS and GA used in synthesis of cryobeads.

2.2.2. Functionalization of CS-based cryobeads

The introduction of ethylenediaminetetraacetic acid (EDTA) ligand moieties onto CS cryobeads was achieved by reaction with EDTAD (Step 2 – Scheme 1) [22]. Thus, 0.15 g of dried cryobeads have been introduced in a round-bottom flask containing 0.6 g EDTAD suspended in 100 mL of acetic acid-methanol (1:1 v/v) mixture and kept under stirring for 24h at 22ºC. Then, the EDTA-functionalized cryobeads were intensively washed with MilliQ water and freeze-dried in a LABCONCO FreeZone apparatus for 48 h, at –50 °C and 0.04 mbars.

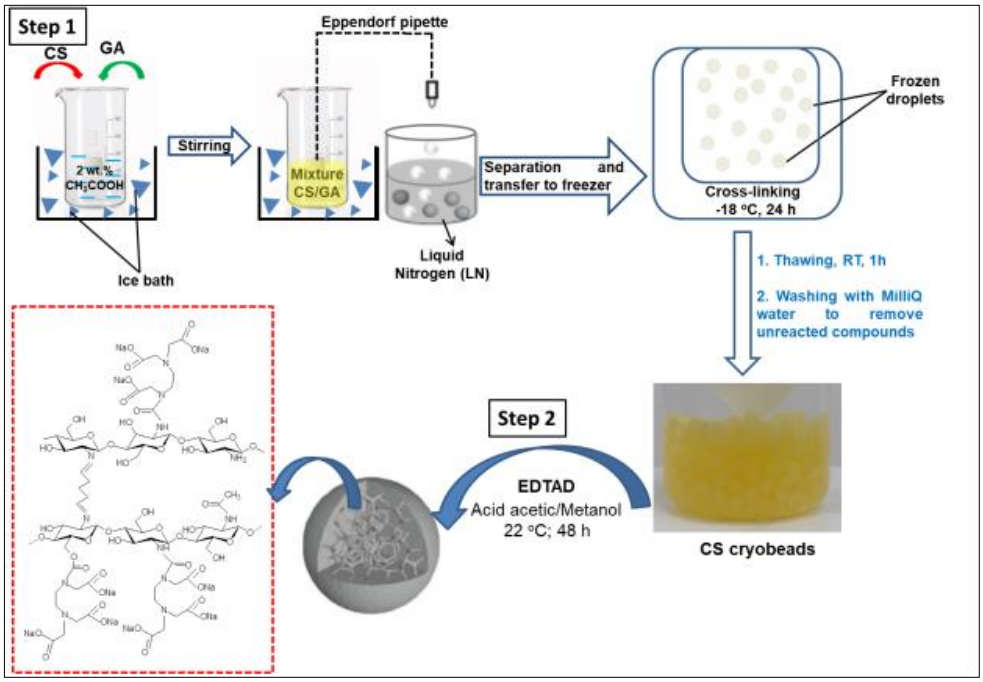

Scheme 1. Schematic illustration of the steps followed for the preparation of CS-based cryogels: Step 1 – formation of CS cryobeads; Step 2 – generation of EDTA ligand groups onto CS cryobeads

2.2.3. Structural and morphological characterization

The FTIR spectra of the CS cryobeads, before and after functionalization with EDTA moieties, were recorded with a Vertex 70 FTIR spectrometer (Bruker, Germany), in the 4000–400 cm^{-1} range, using the KBr tablets. The successful generation of the EDTA ligand groups onto CS matrix was confirmed by proton nuclear magnetic resonance (^{1}H-NMR) spectroscopy, all spectra being registered on a Bruker 400 MHz spectrometer. CS: ^{1}H-NMR (400 MHz, D_2O, *p*H = 1 adjusted with HCl, 25°C, TSP): δ=2.05 ppm (s, 3H; –COC*H*$_3$), 3.18 ppm (s, 1H; –C*H*), 3.41–4.23 ppm (m, 5H; *pyranose ring*), 4.52–4.61 ppm (s, 1H; –CH). The internal morphology of the CS cryobeads was investigated with an Environmental Scanning Electron Microscope (ESEM) type Quanta 200, operating at 20 kV, in low vacuum mode. The mean distance between the channels walls (*MD*, μm) was analyzed by Image J 1.48v software taking into account three independent SEM micrographs for every CS-based sample [38,39]. The overall porosity of the CS cryogels (*P*, *%*) was estimated by the liquid displacement technique, and was calculated by Eq. (2) [4,6].

$$P\ \% = \frac{V_1 - V_3}{V_2 - V_3} x\ 100 \qquad (2)$$

where: V_1 is the initial volume of isopropanol; V_2 is the total volume of isopropanol with the impregnated cryobeads; V_3 is the volume of isopropanol measured after cryobeads separation.

The swelling behavior of CS cryobeads, before and after functionalization with EDTA moieties, was studied in an aqueous solution of *p*H 4 at RT, according to a previously published procedure [4]. The swelling ratio (SR, g/g) was determined by Eq. (3):

$$SR = \frac{w_t}{w_d} \quad (3)$$

where: w_t (g) is the amount of the swollen cryobeads at time t; w_d (g) is the amount of the freeze-dried cryobeads. All data are reported as the average values of three independent experiments.

2.2.4. Sorption/desorption experiments and reusability

The sorption studies of both sorbents were carried out using a copper(II) chloride dehydrate aqueous solution of *p*H 4 by batch system. The sorption kinetics were investigated by adding 10 mL aqueous solution of Cu^{2+} ions with a concentration of 200 mg/L in a flask containing about 0.01 g of freeze-dried cryobeads, and kept in contact at RT for different period of times varying from 5 min to 180 min. The amount of the Cu^{2+} ions retained by CS-based cryobeads at time t, q_t (mg/g) was calculated by Eq. (4):

$$q_t = \frac{(C_0 - C_t) \cdot V}{m} \quad (4)$$

where: C_0 is the initial Cu^{2+} ions concentration (mg/L); C_t is the Cu^{2+} ions concentration at time t (mg/L); V is the volume of Cu^{2+} ions solution (L); m is the sorbent dose (g).

The residual concentration of Cu^{2+} ions was determined by Flame Atomic Absorption Spectrometry (FAAS) using a high-resolution ContrAA 300 Analytik Jena spectrometer at the characteristic maximum wavelength of 324 nm. The removal efficiency (*RE, %*) of Cu^{2+} ions from aqueous solution on both sorbents was determined by Eq. (5):

$$RE = \frac{(C_0 - C_e)}{C_0} x100 \quad (5)$$

where: C_0 has the same meaning as in Eq. (4); C_e is the equilibrium Cu^{2+} ions concentration (mg/L).

The desorption studies of the Cu^{2+}-loaded cryobeads were performed with 0.1 M HCl aqueous solution for 120 min. Then, the CS–based cryobeads were intensively washed with MilliQ water and were regenerated with 0.1 M NaOH aqueous solution for 120 min. After this treatment, the CS-based cryobeads were washed with MilliQ water to neutral before employing them in another cycle of sorption.

3. Results and discussions

3.1. Functionalization of CS with EDTA and formation of CS-based cryobeads

The chemical structure and composition of CS-EDTA polymer obtained using a 'green' procedure (Scheme 2) was confirmed by ^{1}H-NMR (Figure 1).

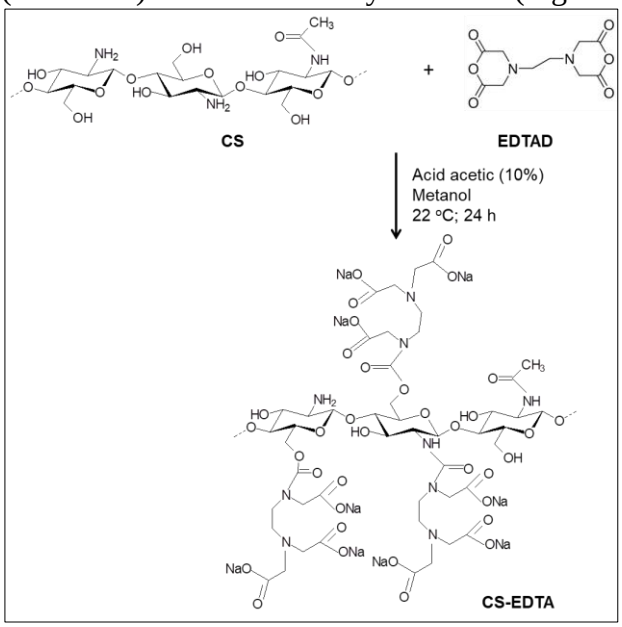

Scheme 2. Functionalization of CS with EDTA ligand groups

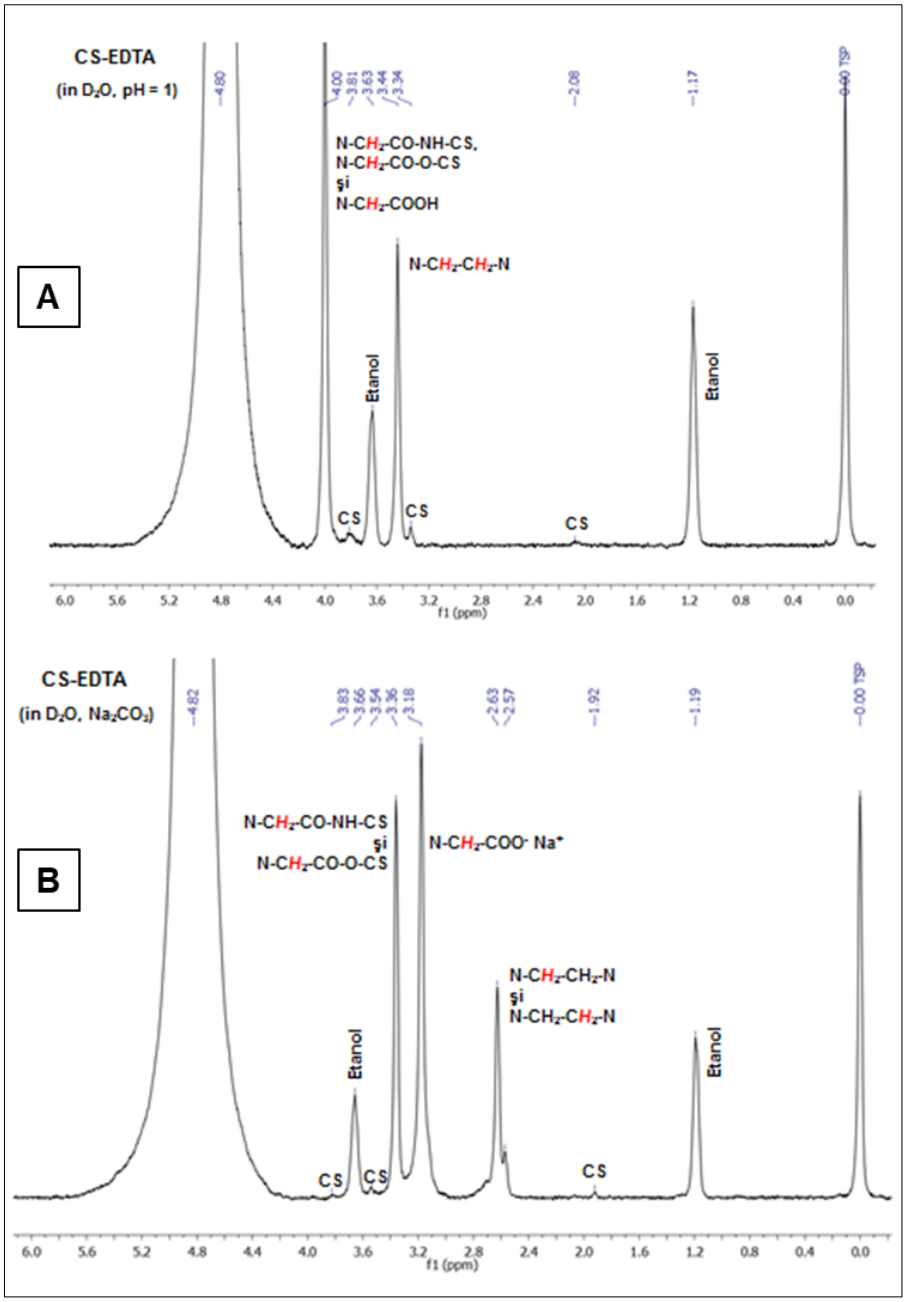

Figure 1. (**A**) ^{1}H-NMR spectrum of CS-EDTA in D_2O adjusted to *p*H 1 with HCl; (**B**) ^{1}H-NMR spectrum of CS-EDTA in D_2O containing a small amount of Na_2CO_3. Both ^{1}H-NMR spectra were registered at 25°C and sodium trimethylsilylpropane sulfonate (TSP) was the internal standard

Herein, the ^{1}H-NMR spectrum of CS-EDTA shows the proton signals specific for EDTA moieties at 3.44 and 4.00 ppm corresponding to the N-CH_2-CH_2-N, N-CH_2-CO-NH-CS, N-CH_2-CO-O-CS, and respectively N-CH_2-COOH groups, besides the characteristic peaks of CS (Figure 1A), being in agreement with the previously published data [27]. In addition, the intense proton signal from 4.00 ppm indicates the reaction of EDTA with both NH_2 and OH groups of CS. Furthermore, in a weak basic medium (Figure 1B), the proton signal from 4.00 ppm was shifted and splited in two distinct peaks at 3.18 ppm and 3.36 ppm, assigned to N-CH_2-COO^-Na^+, N-CH_2-CO-NH-CS gropus, and respectively N-CH_2-CO-O-CS groups. The ^{1}H-NMR data proved the introduction of EDTA ligand groups onto CS according to Scheme 2.

To obtain sorbent materials with high stability during multiple sorption/desorption cycles, the attachment of EDTA ligand groups was further carried out onto cross-linked CS-based cryobeads (Scheme 1 and Figure 2). The images taken by optical microscopy highlighted the spherical shape of the CS-based cryogels and their uniform distribution both in swollen (Figure 2A) and dried state (Figure 2B). In addition, it is observed that the functionalization of the cryogels with EDTA does not affect their shape or integrity. The CS-EDTA cryobeads are more hydrophilic due to the chemically modification of CS with EDTA complexane-type, thus the size diameters in swollen state were around 2.10 mm for CS-EDTA beads and only about 1.80 mm for cross-linked CS beads.

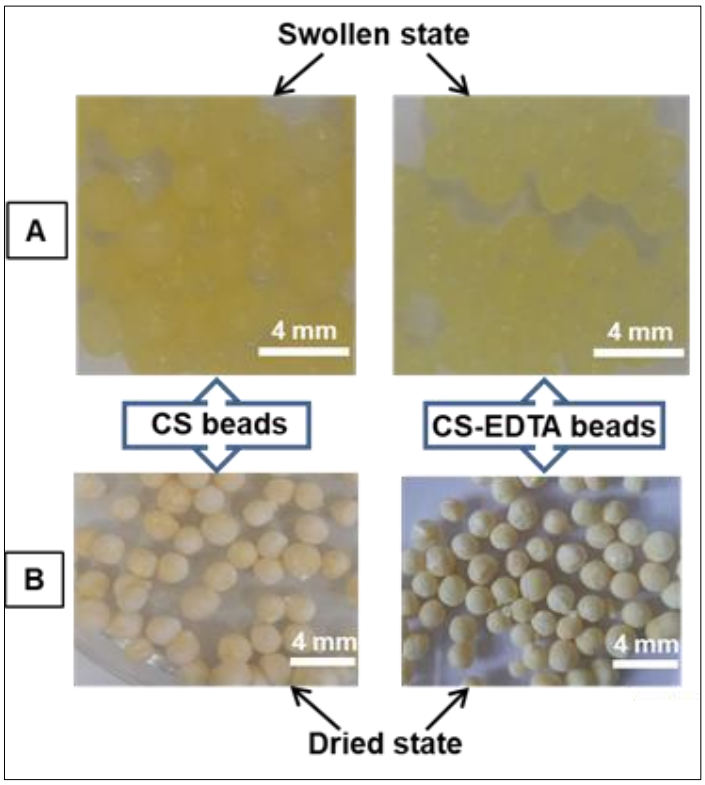

Figure 2. Optical images of cross-linked CS and CS-EDTA Cryobeads in swollen (**A**) and dried state (**B**)

The schematic representation of the synthetic route involved in preparation of EDTA-functionalized sorbents was indicated in Scheme 1. To assess the chemical modifications after CS functionalization, the FTIR spectroscopy was performed. The FTIR spectra of cross-linked CS and CS-EDTA cryobeads are shown in Figure 3.

The characteristic bands at 1660 cm^{-1} attributed to the C=O bond (amide I), 1323 cm^{-1} assigned to the C–N stretching vibration (amide III), and 1598 cm^{-1} corresponding to the NH vibration of NH_2 amide groups (amide II) from the spectrum of CS were either blue-shifted to 1637 cm^{-1} and 1318 cm^{-1} or appeared as a shoulder in the FTIR spectrum of CS-EDTA cryogels (Figure 3). All these shifts and the presence of new peaks in the FTIR spectrum of chemically modified CS at 1738 cm^{-1} and 1394 cm^{-1}, characteristic to the stretching vibration of the C=O bond ester, and respectively to the –COOH groups [16,40], clearly prove the successful modification of CS with EDTA.

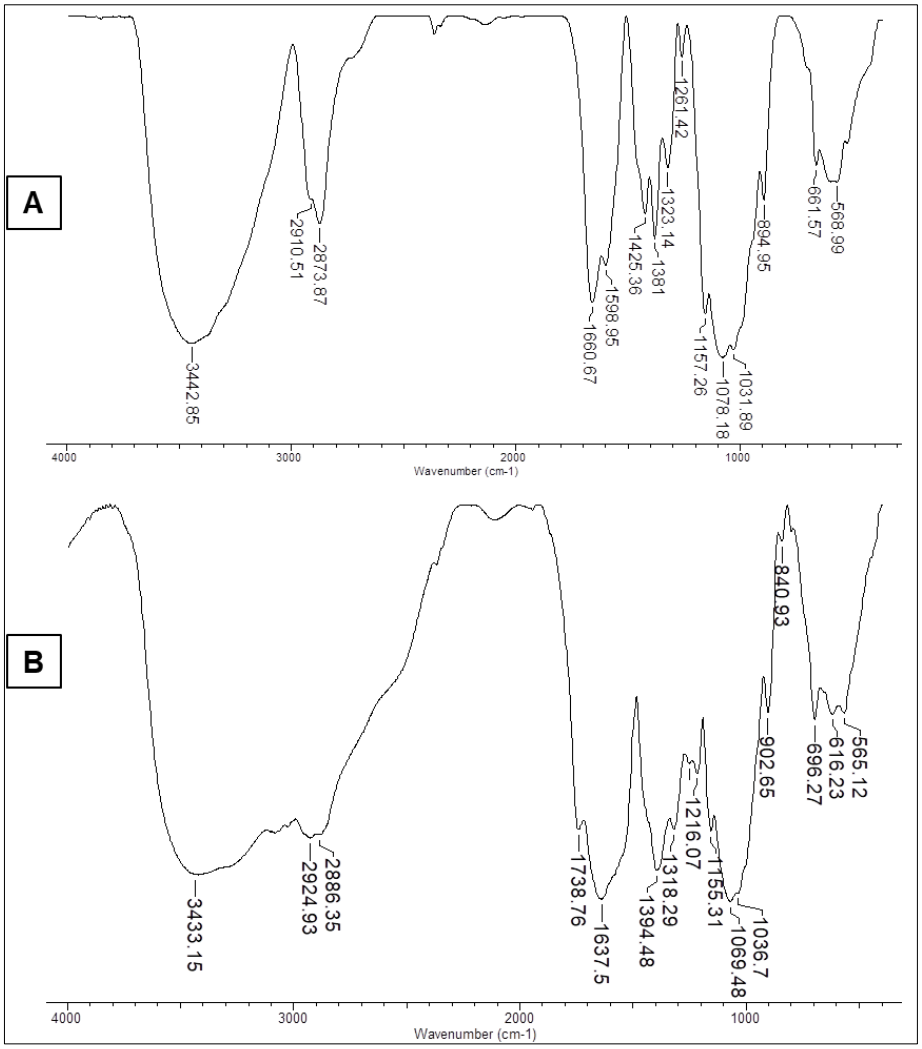

Figure 3. (A) FT-IR spectrum of cross-linked CS; (B) FT-IR spectrum of CS-EDTA cryobeads

The internal morphology of freeze-dried CS-based cryobeads was examined by SEM (Figure 4).

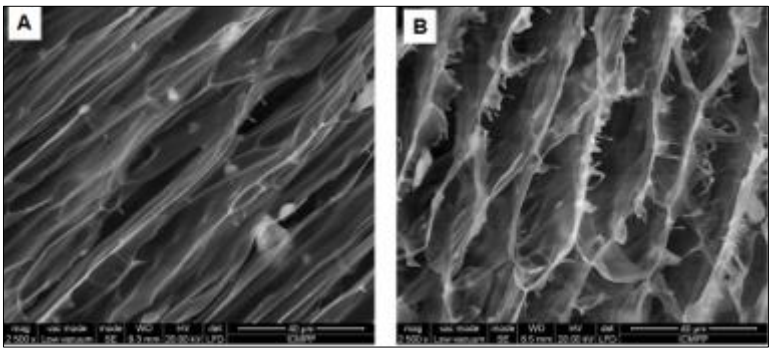

Figure 4. Cross-sectional SEM micrographs of cross-linked CS (A) and CS-EDTA (B) cryogels, the scaling bar is 40 μm while the magnification is 2500x

A porous structure with interconnected lamellar pores oriented by one direction was observed for both cryogel samples with an average distance between the channels walls of 10 ± 2μm for the cross-linked CS (Figure 4A, Table 1) and 14 ± 3 μm for CS-EDTA cryogels (Figure 4B, Table 1). In the case of CS-

EDTA cryogels the pore channel sizes were relatively larger than of unmodified cross-linked CS cryogels (Figure 4). The less compact pore walls of CS-EDTA cryogels demonstrates that the functionalization reaction of cross-linked CS beads took place in the pore walls and not on their surface. The high values of the equilibrium swelling ratio for CS-EDTA cryogels (50 g/g compared with 39 g/g, Table 1) are explained by the presence of the hydrophilic COO^- groups, which further support the successful attachment of EDTA moieties onto CS.

Table 1. Sample codes, gel fraction yield (*GFY, %*), mean distance between the channels walls (*MD*, μm), porosity (*P*, %), and swelling ratio (*SR*, g/g) of CS-based cryobeads

Sample code	[a]GFY, %	[b]MD, μm	[c]P, %	[d]SR, g/g
CS	78.40 ± 1.17	10 ± 2	76.29 ± 2.04	38.92 ± 2.38
CS-EDTA	-	14 ± 3	82.95 ± 2.63	49.88 ± 4.86

[a]*GFY* was calculated by Eq.(1); [b]*MD* was determined from SEM images; [c]*P* was calculated by Eq. (2); [d]*SR* was evaluated gravimetrically using Eq. (3).

The total porosity in dried state (*P, %*) for both samples was evaluated using Eq. (2) and is presented in Table 1. The values of *P* were 76.29 ± 2.04%, and 82.95 ± 2.63%, respectively. The high porosity and the 1D-oriented micro-channeled architecture brought new benefits for CS-based cryobeads facilitating rapid sorption kinetics (Figure 5) in comparison to the CS-based materials, as powders or flakes.

3.2. Sorption studies

The content of HMI released into the environment by different ways continues to increase as a result of both industrial activities and technological development, affecting the normal life of plants, animals and humans, and the finding of efficient and low-cost methods for their removal/recovery is a major concern worldwide. In this context, herein, the CS-based cryobeads were tested for the treatment of copper-containing wastewaters. Figure 5A shows the optical images of cross-linked CS and CS-EDTA cryobeads after interaction with Cu^{2+} ions. As can be observed, the EDTA-functionalized CS-based cryobeads exhibited a more intense green color after the sorption of Cu^{2+} ions, which indicates their higher retention capacity for these HMIs compare to unmodified CS cryobeads. The SEM micrographs taken for both copper-loaded sorbents further sustain the great potential of CS-EDTA cryobeads for removal of Cu^{2+} ions (Figure 5B). The internal morphology of cross-linked CS cryobeads remained almost unchanged, while in the case of CS-EDTA, the pore walls became thicker and the distance between channels walls significantly decreased, which demonstrate a strong interaction between the functional groups of the polymer matrix and Cu^{2+} ions. Consequently, batch-sorption studies were performed to deeply investigate the sorption performance of the CS-EDTA cryobeads in comparison to that of the unmodified CS cryobeads. The influence of contact time (Figure 5C) and number of sorption/desorption cycles (Figure 5D) onto removal of Cu^{2+} ions by CS and CS-EDTA cryobeads were investigated systematically. As Figure 5C shows, the amount of Cu^{2+} ions adsorbed by CS–based cryobeads (CS and CS-EDTA) sharply increased with the increase of contact time from 5 to 30 min, and remained constant afterwards. This fast rate of Cu^{2+} ions sorption by both sorbents can be assigned to the presence of the larger lamellar pores (SEM micrographs, Figure 4) which ensure a rapid diffusion of HMIs to a high number of available functional groups. In addition, the sorption capacity of CS-EDTA cryobeads was about four-times higher than that of unmodified CS cryobeads (168 mg/g compared to 45 mg/g after 30 min, Figure 5C) pointing out the importance of introduction of the EDTA ligand functional groups onto CS matrix. The Cu^{2+} ions retained by our sorbents were successfully desorbed with 0.1 M HCl solution. The CS-EDTA cryobeads were adequately regenerated with 0.1 M NaOH and their feasibility in successive sorption/desorption cycles was analyzed. As can be seen from Figure 5D, the sorption capacity and removal efficiency of CS-EDTA cryobeads were preserved almost constant even after the 10^{th} cycle of sorption/desorption, displaying their extraordinary chemical structure stability.

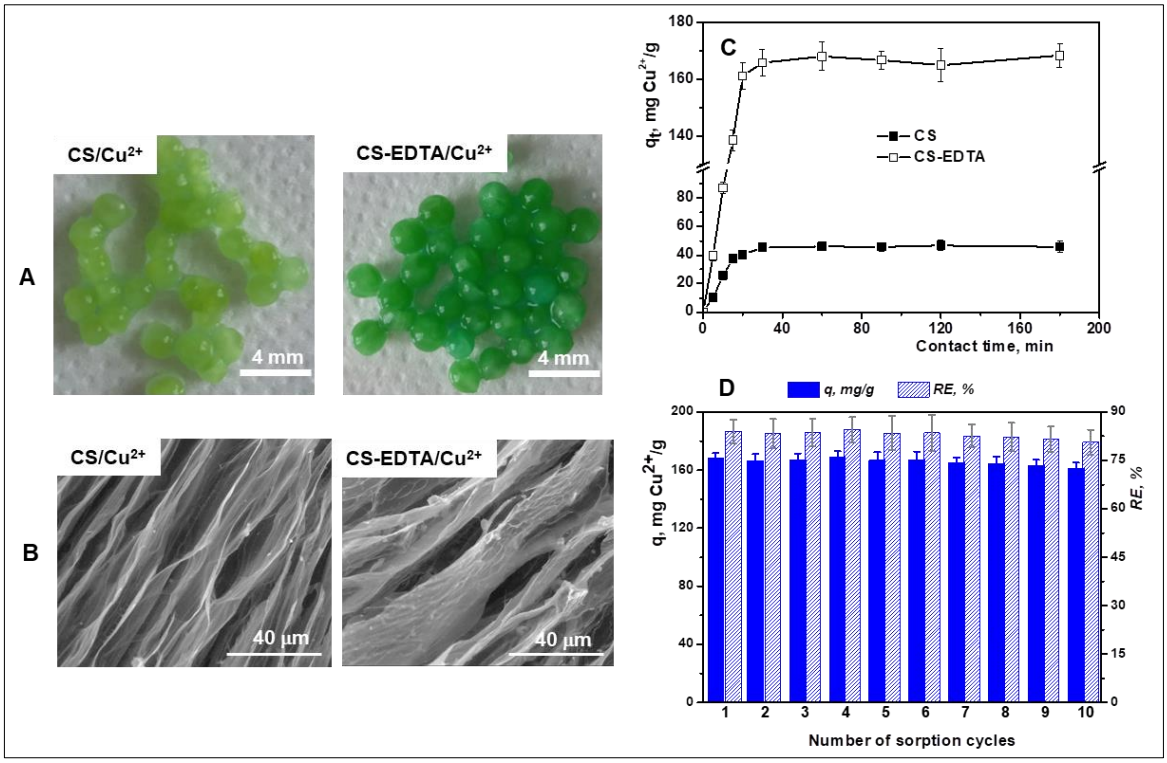

Figure 5. (A) Optical images of Cu^{2+}-loaded onto cross-linked CS and CS-EDTA cryobeads; (B) SEM micrographs of CS-based sorbents after interaction with Cu^{2+} ions; (C) Effect of contact time onto Cu^{2+} ions retention from aqueous solution by CS and CS-EDTA cryobeads; (D) Sorption capacity (*q*, mg/g) and removal efficiency (*RE*, %) as a function of several consecutive sorption/desorption cycles

EDTA-modified CS derivatives have been tested before only for the removal of Pb(II) [21,25,28], Ni(II) [22,23], and Co(II) [23], or for the chromatographic separation of rare earths [24]. The usage of water soluble EDTA-linked CS as a flocculant for Cu(II) ions has been also evaluated [27]. However, this study reports for the first time preparation of EDTA-functionalized CS cryogels with a strong chelation capability and a broaden 'active' surface area for binding Cu(II) ions. The comparison of our sorption data with other previously published sorbents indicate the high potential of these cryogels in remediation of wastewaters containing Cu^{2+} ions (Table 2).

Table 2. Functionalized CS sorbents for the removal of Cu^{2+} ions from aqueous solutions.

Sorbent	Sorption Capacity,[a] mg/g	pH	Dose of sorbent, g/L	Equilibrium time, min	Desorption and reusability	Reference
Bifunctionalized CS (C2)	71.5	4.5	0.2	360	22.4% desorption	[41]
Bifunctionalized CS (C4)	165.2	5.5	0.2	240	incomplete desorption	[42]
CS hydrogel beads	163.9	4	5	1440	ND[b]	[11]
Thiourea-*g*-CS hydrogels	129.8	5	1.2	1440	complete regeneration and re-use in 3 cycles of sorption/desorption	[20]
EDTA-CS-CMC[c]	142.95	5.5	-	40	complete regeneration and re-use in 5 cycles of sorption/desorption	[43]
CS-EDTA cryogels	168	4	1	30	complete regeneration and re-use in 10 cycles of sorption/desorption	This study

[a]All sorption experiments were performed at 25 °C; [b]ND – not determined; [c]CMC - carboxymethyl cellulose.

Thus, the CS-EDTA cryobeads exhibited a comparable or even higher sorption capacity than the other CS-modified sorbents. In addition, these cryogel sorbents required only 30 min to completely remove the Cu^{2+} ions and were successfully desorbed and re-used in 10 consecutive cycles of sorption/desorption without a significant loss of sorption capacity, which recommend them as remarkable bio-sorbents in treatment of HMIs-containing wastewaters.

4. Conclusions

In this study, the functionalization with EDTA of both CS and cross-linked CS cryobeads was successfully achieved. The chemical structure of CS before and after modification with EDTA groups was highlighted by FTIR and ^{1}H-NMR spectroscopy. A 1D-oriented porous structure with lamellar interconnected pores was observed for both sorbents, i.e. cross-linked CS and CS-EDTA cryobeads. The sorption studies revealed that the CS-EDTA cryobeads exhibited a sorption capacity of 168 mg/g, which is four-times higher than that of unmodified cryobeads. The fast kinetic rate, the remarkable reusability as well as the low-cost production of the CS-EDTA cryobeads, clearly indicate their huge potential for removal of HMIs from contaminated waters.

Acknowledgments: This work was supported by a grant of Romanian Ministry of Research and Innovation (CCCDI-UEFISCDI) PN-III-P1-1.1-TE-2016-1697 project [TE117/10.10.2018].

References

1. CRINI, G., Recent Developments in Polysaccharide-Based Materials Used as Adsorbents in Wastewater Treatment, *Prog. Polym. Sci*., **30**(1), 2005, 38-70.
2. DESBRIÈRES, J., GUIBAL, E., Chitosan for Wastewater Treatment, *Polym. Int*., **67**(1), 2018, 7-14.
3. PAKDEL, P.M., PEIGHAMBARDOUST, S.J., Review on Recent Progress in Chitosan-Based Hydrogels for Wastewater Treatment Application, *Carbohydr. Polym.*, **201**(1), 2018, 264-279.
4. SÁEZ, P., DINU, I.A., RODRÍGUEZ, A., GÓMEZ, J.M., LAZAR, M.M., ROSSINI, D., DINU, M.V., Composite Cryo-beads of Chitosan Reinforced with Natural Zeolites with Remarkable Elasticity and Switching on/off Selectivity for Heavy Metal Ions, *Int. J. Biol. Macromol*., **164**, 2020, 2432-2449.
5. DINU, M.V., DINU, I.A., LAZAR, M.M., DRAGAN, E.S., Insights Into the Mechanism of Cu^{2+} Binding onto Chitosan-Based Cryogel Composites: Equilibrium, Kinetic and Thermodynamic Studies, *Cellulose Chem. Technol*., **52**(3-4), 2018, 181-192.
6. HUMELNICU, D., DRAGAN, E.S., DINU, M.V., A Comparative Study on Cu^{2+}, $Zn^{2+,}$ Ni^{2+}, Fe^{3+}, and Cr^{3+} Metal Ions Removal by Chitosan-Based Composite Cryogels, *Molecules*, **25**(11), 2020, 2664.
7. DINU, M.V., LAZAR, M.M., DRAGAN, E.S., Dual Ionic Cross-Linked Alginate/Clinoptilolite Composite Microbeads with Improved Stability and Enhanced Sorption Properties for Methylene Blue, *React. Funct. Polym*., **116**, 2017, 31-40.
8. QI, X., ZENG, Q., TONG, X., SU, T., XIE, L., YUAN, K., XU, J., SHEN J., Polydopamine/ Montmorillonite-Embedded Pullulan Hydrogels as Efficient Adsorbents for Removing Crystal Violet, *J. Hazard. Mater*., **402**, 2021, 123359.
9. DRAGAN, E.S., HUMELNICU, D., DINU, M.V., Development of Chitosan-Poly(ethyleneimine) Based Double Network Cryogels and Their Application as Superadsorbents for Phosphate, *Carbohydr. Polym*. **210**, 2019, 17-25.
10. DINU, I.A., GHIMICI, L., Removal of Some Commercial Pesticides from Aqueous Dispersions Using as Flocculant a Thymine-Containing Chitosan Derivative, *Sep. Purif. Technol*., **209**, 2019, 698–706.
11. LI, N., BAI, R., A Novel Amine-Shielded Surface Cross-linking of Chitosan Hydrogel Beads for Ehanced Metal Adsorption Performance, *Ind. Eng. Chem. Res*., **44**(17), 2005, 6692-6700.
12. KAMINSKI, W., TOMCZAK, E., JAROS, K., Interactions of Metal Ions Sorbed on Chitosan Beads, *Desalination*, **218**(1), 2008, 281-286.

13. BRATSKAYA, S., PRIVAR, Y., NESTEROV, D., MODIN, E., KODESS, M.I., SLOBODYUK, A., MARININ, D.V., PESTOV, A.V., Chitosan Gels and Cryogels Cross-linked with Diglycidyl Ethers of Ethylene Glycol and Polyethylene Glycol in Acidic Media, *Biomacromolecules*, **20**(4), 2019, 1635–1643.
14. DRAGAN, E.S., DINU, M.V., Advances in Porous Chitosan-Based Composite Hydrogels: Synthesis and Applications, *React. Funct. Polym*., **146**, 2020, 104372.
15. UPADHYAY, U., SREEDHAR, I., SINGH, S.A., PATEL, C.M., ANITHA, K.L., Recent Advances in Heavy Metal Removal by Chitosan Based Adsorbents, *Carbohdr. Polym*., **251**, 2021, 117000.
16. ZHUANG, S., CHENG, R., KANG, M., WANG, J., Kinetic and Equilibrium of U(VI) Adsorption onto Magnetic Amidoxime-Functionalized Chitosan Beads, *J. Clean. Prod*., **188**, 2018, 655-661.
17. ANIRUDHAN, T.S., LEKSHMI, G.S., SHAINY, F., Synthesis and Characterization of Amidoxime Modified Chitosan/Bentonite Composite for the Adsorptive Removal and Recovery of Uranium from Seawater, *J. Colloid Interf. Sci*., **534**, 2019, 248-261.
18. HAMZA, M.F., ROUX, J.C., GUIBAL, E., Uranium and Europium Sorption on Amidoxime-Functionalized Magnetic Chitosan Micro-Particles, *Chem. Eng. J*., **344**, 2018, 124-137.
19. MOZAFFARI, M., EMAMI, M.R.S., BINAEIAN, E., A Novel Thiosemicarbazide Modified Chitosan (TSFCS) for Efficiency Removal of Pb (II) and Methyl Red from Aqueous Solution, *Int. J. Biol. Macromol*., **123**, 2019, 457-467.
20. GHIORGHITA, C.A., BORCHERT, K.B.L., VASILIU, A.L., ZAHARIA, M.M., SCHWARZ, D., MIHAI, M., Porous Thiourea-Grafted-Chitosan Hydrogels: Synthesis and Sorption of Toxic Metal Ions from Contaminated Waters, *Colloids Surf. A*, **607**, 2020, 125504.
21. INOUE, K., OHTO, K., YOSHIZUKA, K., YAMAGUCHI, T., TANAKA, T., Adsorption of Lead(II) Ion on Complexane Types of Chemically Modified Chitosan, *Bull. Chem. Soc. Jpn*., **70**(10), 1997, 2443-2447.
22. NAGIB, S., INOUE, K., YAMAGUCHI, T., TAMARU, T., Recovery of Ni from a Large Excess of Al Generated from Spent Hydrodesulfurization Catalyst using Picolylamine Type Chelating Resin and Complexane Types of Chemically Modified Chitosan, *Hydrometallurgy*, **51**(1), 1999, 73-85.
23. REPO, E., WARCHOL, J.K., KURNIAWANA, T.A., SILLANPÄÄ, M.E.T., Adsorption of Co(II) and Ni(II) by EDTA- and/or DTPA-Modified Chitosan: Kinetic and Equilibrium Modeling, *Chem. Eng. J*., **161**(1-2), 2010, 73-82.
24. ROOSEN, J., BINNEMANS, K., Adsorption and Chromatographic Separation of Rare Earths with EDTA- and DTPA-Functionalized Chitosan Biopolymers, *J. Mater. Chem. A*, **2**(5),2014, 1530-1540.
25. AYATI, A., TANHAEI, B., SILLANPAA, M., Lead(II)-Ion removal by Ethylenediaminetetraacetic Acid Ligand Functionalized Magnetic Chitosan–Aluminum Oxide–Iron Oxide Nanoadsorbents and Microadsorbents: Equilibrium, Kinetics, and Thermodynamics, *J. Appl. Polym. Sci*., **134**(4), 2017, 44360.
26. SHENG, L., ZHOU, L., HUANG, Z., LIU, Z., CHEN, Q., HUANG, G., ADESINa, A.A., Facile Synthesis of Magnetic Chitosan Nano-Particles Functionalized with N/O-Containing Groups for Efficient Adsorption of U(VI) from Aqueous Solution, *J. Radioanal Nucl. Chem.*, **310**(3), 2016, 1361-1371.
27. FUJITA, S., SAKAIRI, N., Water Soluble EDTA-Linked Chitosan as a Zwitterionic Flocculant for *p*H Sensitive Removal of Cu(II) ion, *RSC Adv*., **6**(13), 2016, 10385-10392.
28. KHAWAR, A., ASLAM, Z., ABBAS, S.J.A., Pb (II) Biosorption Using DAP/EDTA-Modified Biopolymer (Chitosan), *Chem. Eng. Commun*., **205**(11), 2018, 1555-1567.
29. GUO, D.M., AN, Q.D., XIAO, Z.Y., ZHAI, S.R., YANG, D.J., Efficient Removal of Pb(II), Cr(VI) and Organic Dyes by Polydopamine Modified Chitosan Aerogels, *Carbohydr. Polym*., **202**, 2018, 306-314.
30. IMAMA, E.A., EL-SAYED, I.E.T., MAHFOUZ, M.G., TOLBA, A.A., AKASHI, T., GALHOUM, A.A., GUIBAL, E., Synthesis of α-Aminophosphonate Functionalized Chitosan Sorbents: Effect of Methyl vs Phenyl Group on Uranium Sorption, *Chem. Eng. J*., **352**, 2018, 1022-1034.

31. NIE, J., PEI, B., WANG, Z., HU, Q., Construction of Ordered Structure in Polysaccharide Hydrogel: A review, *Carbohydr. Polym*., **205**, 2019, 225–235.
32. MEMIC, A., COLOMBANI, T., EGGERMONT, L.J., REZAEEYAZDI, M., STEINGOLD, J., ROGERS, Z.J., NAVARE, K.J., MOHAMMED, H.S, BENCHERIF, S.A., Latest Advances in Cryogel Technology for Biomedical Applications, *Adv. Therap*., **2**(4), 2019, 1800114.
33. LOZINSKY, V.I., Cryostructuring of Polymeric Systems. 55. Retrospective View on the More than 40 Years of Studies Performed in the A.N. Nesmeyanov Institute of Organoelement Compounds with Respect of the Cryostructuring Processes in Polymeric Systems, *Gels*, **6**, 2020, 29.
34. HUMELNICU, D., LAZAR, M.M., IGNAT, M., I.A., DINU, E.S. DRAGAN, M.V. DINU, Removal of Heavy Metal Ions from Multi-Component Aqueous Solutions by Eco-Friendly and Low-Cost Composite Sorbents with Anisotropic Pores, *J. Hazard. Mater*., **38**, 2020, 120980.
35. KASAAI, M.R., Determination of the Degree of N-Acetylation for Chitin and Chitosan by Various NMR Spectroscopy Techniques: A review, *Carbohydr. Polym*., **79**(4), 2010, 801-810.
36. GAMZAZADE, A.I., SHIMAC, V.M., SKLJAR, A.M., STYKOVA, E.V., PAVLOVA, S.A., ROGOZIN, S.V., Investigation of the Hydrodynamic Properties of Chitosan Solutions, *Acta Polymerica*, **36**(8), 1985, 420-424.
37. ORAKDOGEN N., Novel Responsive Poly(N,N-Dimethylaminoethyl Methacrylate) Gel Beads: Preparation, Mechanical Properties and pH-Dependent Swelling Behavior, *J. Polym. Res*., **19**, 2012, 9914.
38. RASCHIP, I.E., FIFERE, N., VARGANICI, C.D., DINU, M.V., Development of Antioxidant and Antimicrobial Xanthan-Based Cryogels with Tuned Porous Morphology and Controlled Swelling Features, *Int. J. Biol. Macromol*., **156**, 2020, 608–620.
39. LAZAR, M.M., DINU, I.A., SILION, M., DRAGAN, E.S., DINU, M.V., Could the Porous Chitosan-Based Composite Materials Have a Chance to a "NEW LIFE" After Cu(II) Ion Binding? *Int. J. Biol. Macromol*., **131**, 2019, 134–146.
40. MOYO, M., PAKADE, V.E., MODISE, S.J., Biosorption of Lead(II) by Chemically Modified Mangifera Indica Seed Shells: Adsorbent Preparation, Characterization and Performance Assessment, *Process Saf. Environ*., **111**, 2017, 40-51
41. ALMEIDA, R.F.T., FERREIRA, B.C.S., MOREIRA, A.L.S.L., FREITAS, R.P., GIL, L.F., GURGE, L.V.A., Application of a new bifunctionalized chitosan derivative with zwitterionic characteristics for the adsorption of Cu^{2+}, Co^{2+}, Ni^{2+}, and oxyanions of Cr^{6+} from aqueous solutions: Kinetic and equilibrium aspects, *J. Colloid Interface Sci*., **466**, 2016, 297-309.
42. MOREIRA, A.L.S.L., PEREIRA, A.S., SPEZIALI, M.G., NOVACK, K.M., GURGEL, L.V.A., GIL, L.F., Bifunctionalized chitosan: A versatile adsorbent for removal of Cu(II) and Cr(VI) from aqueous solution, *Carbohydr. Polym*., **201**, 2018, 218–227.
43. MANZOOR, K., AHMAD, M., AHMAD, S., IKRAM, S., Synthesis, characterization, kinetics, and thermodynamics of EDTA-modified chitosan-carboxymethyl cellulose as Cu(II) ion adsorbent, *ACS Omega*, **4**, 2019, 17425–17437.

Manuscript received: 18.01.2021